AD-A077 558 POLYTECHNIC INST OF NEW YORK FARMINGDALE DEPT OF MEC--ETC F/G 20/4
NUMERICAL INTEGRATION OF COMPRESSIBLE, VISCOUS FLOW EQUATIONS.(U)
SEP 79 G MORETTI
UNCLASSIFIED POLY-M/AE-79-40 ARO-14369.3-E DAAG29-77-G-0072 NL

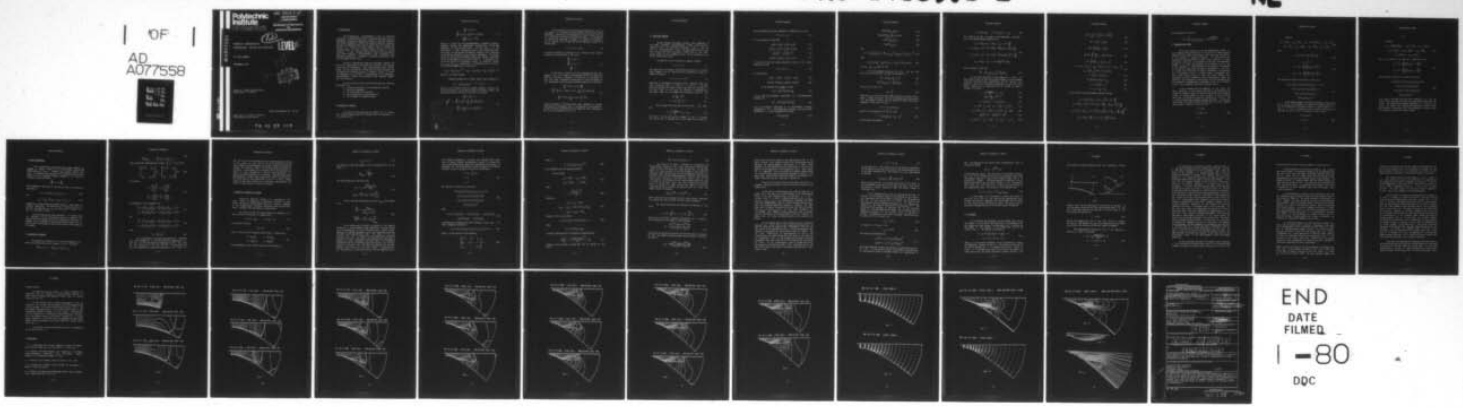

END
DATE FILMED
1-80
DDC

Polytechnic Institute of New York

AERODYNAMICS LABORATORIES
~
DEPARTMENT OF MECHANICAL and AEROSPACE ENGINEERING

12

LEVEL II

NUMERICAL INTEGRATION OF COMPRESSIBLE, VISCOUS FLOW EQUATIONS

by GINO MORETTI

SEPTEMBER 1979

Grant No. DAAG 29-77-G-0072
Project No. P 14369-E

POLY M/AE Report No. 79-40

1. Introduction

Multi-dimensional, time-dependent flows are generally considered as problems which can be analyzed numerically only by high-speed, large-scale computers, because of the large number of grid points necessary to achieve the required degree of accuracy. The need is emphasized when viscous effects have to be taken into account [1]. There is no doubt, however, that the inclusion of viscous effects is a must to achieve physical reality in certain problems. To this category belong all flows involving separation, plume formation, shock-boundary layer interaction with upstream propagation of signals in a generally supersonic flow, self-sustained flutter, etc.

The use of appropriate numerical techniques reduces the need for a large number of grid points and allows a mini-computer to be used for the analysis. After experimenting with a certain number of such problems and finding that the above statement can be supported by concrete evidence, I consider proper to report the techniques in full detail. Two-dimensional or axi-symmetric, time-dependent, viscous flow problems at high Reynolds numbers will be considered.

We will discuss the basic points which make the technique efficient, viz.:

a) a proper formulation of the equations of motion,
b) the use of mappings,
c) the stretching of coordinates,
d) the discretization of the equations,
e) the treatment of imbedded shocks.

2. Equations of motion

In vector form, the equations of motion for a viscous flow (Navier-Stokes equations), assuming that the viscosity, μ, is a constant, are:

Equations of motion

$$\frac{D\rho}{Dt} + \rho\nabla.\vec{V} = 0$$

$$\frac{D\vec{V}}{Dt} + \frac{1}{\rho}\nabla p = \frac{4}{3}\frac{\mu}{\rho}\nabla\nabla.\vec{V} - \frac{\mu}{\rho}\nabla\times\nabla\times\vec{V} \qquad (1)$$

$$\rho\theta\frac{DS}{Dt} = \mu\Phi + \kappa\nabla^2\theta$$

where ρ, p, S and θ are the thermodynamical parameters density, pressure, entropy and temperature, respectively. In the same equations, $\vec{V}$ is the velocity vector, t is the time, κ is the coefficient of heat conduction, and Φ is the dissipation term. The latter is a well-known non-negative quadratic form depending on the space derivatives of the velocity components. Its expressions for the various orthogonal coordinate systems considered in the present Report will be given later on. If pressures, densities and lengths are expressed in terms of reference values, p_{ref}, ρ_{ref} and x_{ref}, respectively, corresponding units of velocity, time and temperature are defined as

$$u_{ref} = (p_{ref}/\rho_{ref})^{1/2}, \quad t_{ref} = x_{ref}/u_{ref}, \quad \theta_{ref} = u_{ref}^2/R \qquad (2)$$

where R is the gas constant.

A Reynolds number and a Prandtl number can be defined as

$$R_e = \rho_{ref}u_{ref}x_{ref}/\mu, \qquad P_r = c_p\mu/\kappa$$

where c_p is the specific heat at constant pressure. Finally, let the unit entropy be c_v (the specific heat at constant volume). The equations of motion can thus be written in the form:

$$\frac{D\rho}{Dt} + \rho\nabla.\vec{V} = 0$$

$$\frac{D\vec{V}}{Dt} + \frac{1}{\rho}\nabla p = \frac{1}{\rho R_e}\left[\frac{4}{3}\nabla\nabla.\vec{V} - \nabla\times\nabla\times\vec{V}\right] \qquad (3)$$

$$\frac{DS}{Dt} = \frac{1}{p\,R_e}\left[(\gamma-1)\Phi + \frac{\gamma}{P_r}\nabla^2\theta\right]$$

In an inviscid flow, the terms here affected by $1/R_e$ do not appear. For a proper numerical analysis of such flows, whose mechanics is governed by the propagation of sound waves and by the convection of entropy along particle paths, it is convenient to consider the logarithm of pressure, P, instead of the density, as an unknown, and to make use of the equation of state for a perfect gas:

$$S = \gamma \ln \theta - (\gamma-1)P \tag{4}$$

so that the equations of motion for an inviscid flow (Euler's equations) can be written in the form:

$$\begin{aligned} &\frac{DP}{Dt} + \gamma \nabla.\vec{V} = 0 \\ &\frac{D\vec{V}}{Dt} + \theta \nabla P = 0 \\ &\frac{DS}{Dt} = 0 \end{aligned} \tag{5}$$

If the flow is viscous, the basic phenomena of wave propagation are still present, although modified by the concurrent effects of diffusion. Therefore, it would not be advisable to drop the basic integration techniques for convective terms; we will consequently write the Navier-Stokes equations in the form:

$$\begin{aligned} &\frac{\partial P}{\partial t} + \vec{V}.\nabla P + \gamma \nabla.\vec{V} = \frac{DS}{Dt} \\ &\frac{\partial \vec{V}}{\partial t} + \frac{1}{2}\nabla(q^2) - \vec{V}\times\nabla\times\vec{V} + \theta \nabla P = \frac{1}{\rho R_e}\left[\frac{4}{3}\nabla\nabla.\vec{V} - \nabla\times\nabla\times\vec{V}\right] \\ &\frac{\partial S}{\partial t} + \vec{V}.\nabla S = \frac{1}{\rho R_e}\left[(\gamma-1)\Phi + \frac{\gamma}{P_r}\nabla^2\theta\right] \end{aligned} \tag{6}$$

(where the material derivatives have been replaced by partial derivatives, as costumary, and q is the modulus of the velocity). In what follows, the density will no longer be used explicitly, and ρ will be redefined in Eq. (8).

3. Conformal mapping

We will consider two types of flows, both depending on two space variables: two-dimensional (plane) flows and axi-symmetric flows. Two Cartesian coordinates, x and y, will be used for two-dimensional flows. the same symbols will be used for the axial and radial coordinate, respectively, in any meridional plane of an axi-symmetric flow. The (x,y)-plane will be called the physical plane.

In addition, we will introduce a complex variable

$$z = x + i\, y \tag{7}$$

and assume that, in general, the physical plane will be conformally mapped onto an auxiliary plane, described in terms of a complex variable ζ,

$$\zeta = \xi + i\, \eta = \rho\, e^{i\theta} \tag{8}$$

Obviously, if no mapping is needed, all the formulas below are valid, provided that $\zeta = z$, that is, $\xi = x$ and $\eta = y$. The mapping function must be chosen in such a way that the contours of the flow field are as close as possible to ξ=constant and η=constant lines, or to ρ=constant and θ=constant lines [2]. Let

$$g = \frac{d\zeta}{dz} = G e^{i\omega} \tag{9}$$

$$\mathcal{C} + i\, \mathcal{S} = \frac{G}{g} = e^{-i\omega} \tag{10}$$

We will begin with the case in which ξ and η are used. Let

$$\phi = \frac{1}{g}\frac{d \log g}{dz} = \phi_1 + i\, \phi_2 \tag{12}$$

Let also $\hat{\imath}$, $\hat{\jmath}$ be the unit vectors tangent to the η = constant line and to the ξ = constant line in the z-plane, and u and v be

the corresponding velocity components, respectively, so that

$$\vec{V} = u\,\hat{\imath} + v\,\hat{\jmath} \tag{13}$$

It is convenient to note that

$$\xi_x = G\ell,\ \xi_y = G\mathcal{B},\ \eta_x = -G\mathcal{B},\ \eta_y = G\ell \tag{14}$$

$$x_\xi = \ell/G,\ x_\eta = -\mathcal{B}/G,\ y_\xi = \mathcal{B}/G,\ y_\eta = \ell/G \tag{15}$$

$$\xi_x^2 + \xi_y^2 = G^2,\quad x_\xi^2 + x_\eta^2 = 1/G^2 \tag{16}$$

$$G_\xi = G\phi_1,\ G_\eta = -G\phi_2,\ \omega_\xi = \phi_2,\ \omega_\eta = \phi_1 \tag{17}$$

If $\hat{\imath}$ and $\hat{\jmath}$ are the unit vectors parallel to the x- and y-axis, respectively, and

$$\vec{V} = U\,\hat{\imath} + V\,\hat{\jmath} \tag{18}$$

it follows that

$$\hat{\imath}.\hat{\imath} = \ell\ ,\quad \hat{\imath}.\hat{\jmath} = \mathcal{B}\ ,\quad \hat{\jmath}.\hat{\imath} = -\mathcal{B}\ ,\quad \hat{\jmath}.\hat{\jmath} = \ell \tag{19}$$

$$U = u\ell - v\mathcal{B},\ V = u\mathcal{B} + v\ell,\ u = U\ell + V\mathcal{B},\ v = -U\mathcal{B} + V\ell \tag{20}$$

For any element ds <u>in space</u>, we have

$$ds^2 = d\xi^2/G^2 + d\eta^2/G^2 + dx_3^2 \tag{21}$$

if x_3 is the third Cartesian coordinate, in a two-dimensional problem, and

$$ds^2 = d\xi^2/G^2 + d\eta^2/G^2 + y^2 dx_3^2 \tag{22}$$

if x_3 is the angular coordinate in an axi-symmetric problem. Consequently, in a two-dimensional problem, the basic vector operators in (1) can be expressed as follows:

$$\nabla P = G(P_\xi\,\hat{\imath} + P_\eta\,\hat{\jmath}) \tag{23}$$

$$\nabla\times\vec{V}=G^2[(\frac{v}{G})_\xi-(\frac{u}{G})_\eta]\hat{k} \tag{24}$$

$$\vec{V}\times\nabla\times\vec{V}=G^2[(\frac{v}{G})_\xi-(\frac{u}{G})_\eta](v\hat{i}-u\hat{j}) \tag{25}$$

$$\nabla.\vec{V}=G^2[(\frac{u}{G})_\xi+(\frac{v}{G})_\eta] \tag{26}$$

$$\nabla^2\theta=G^2(\theta_{\xi\xi}+\theta_{\eta\eta}) \tag{27}$$

and

$$\Phi = 4(e_{12}^2+e_{23}^2+e_{31}^2) + \frac{2}{3}[(e_{11}-e_{22})^2+(e_{22}-e_{33})^2+(e_{33}-e_{11})^2] \tag{28}$$

with

$$e_{11}=G(u_\xi+v\phi_2),\ e_{22}=G(v_\eta-u\phi_1),\ e_{12}=\frac{1}{2}[(Gv)_\xi+(Gu)_\eta] \tag{29}$$

and e_{33}, e_{23}, e_{31} equal to zero.

In an axi-symmetric problem, (23), (24), (25) and (28) still hold, but (26) and (27) must be replaced by

$$\nabla.\vec{V} = G^2[(\frac{u}{G})_\xi+(\frac{v}{G})_\eta] + \frac{V}{y} \tag{30}$$

$$\nabla^2\theta=G^2(\theta_{\xi\xi}+\theta_{\eta\eta}) + \frac{G}{y}(\beta\theta_\xi+\gamma\theta_\eta) \tag{31}$$

and e_{33} is not zero, but

$$e_{33} = \frac{V}{y} \tag{32}$$

From now on, we will follow the common practice of using a multiplier, j, which is equal to zero for two-dimensional flows and to 1 for axi-symmetric flows. We will denote by Ω the only non-zero component of the curl of $\vec{V}$ (24):

$$\Omega = G\ (v_\xi-u_\eta-v\phi_1-u\phi_2) \tag{33}$$

and by Δ the divergence of $\vec{V}$ (26) or (30):

$$\Delta = e_{11}+e_{22}+e_{33},\quad e_{33} = j\frac{V}{y} \tag{34}$$

and introduce the symbols

$$D = G(v\phi_1 + u\phi_2) \ , \quad E = G(v\phi_2 - u\phi_1) + e_{33} \tag{35}$$

It is easy to see that, in terms of the independent variables ξ and η, the Navier-Stokes equations are:

$$\begin{aligned}
&P_t + G(uP_\xi + vP_\eta) + \gamma G(u_\xi + v_\eta) + \gamma E = \frac{DS}{Dt} \\
&u_t + G(uu_\xi + vu_\eta) + vD + G\theta P_\xi = [\tfrac{4}{3}G\Delta_\xi - G\Omega_\eta - j\frac{\ell}{y}\Omega]\frac{\theta}{pR_e} \\
&v_t + G(uv_\xi + vv_\eta) - uD + G\theta P_\eta = [\tfrac{4}{3}G\Delta_\eta + G\Omega_\xi + j\frac{\mathcal{S}}{y}\Omega]\frac{\theta}{pR_e} \\
&S_t + G(uS_\xi + vS_\eta) = [(\gamma-1)\Phi + \frac{\gamma}{P_r}\nabla^2\theta]/(pR_e)
\end{aligned} \tag{36}$$

with Φ defined by (28) and

$$\nabla^2\theta = G^2(\theta_{\xi\xi} + \theta_{\eta\eta}) + j\frac{G}{y}(\mathcal{S}\theta_\xi + \ell\theta_\eta) \tag{37}$$

If the basic variables in the ζ-plane are ρ and θ, we will define $\hat{\imath}$ and $\hat{\jmath}$ as the unit vectors tangent to the θ=constant lines and ρ=constant lines, respectively, and the velocity components, u and v, will be defined accordingly, so that (13) still holds. Practically, all equations from (12) through (37) must be changed, as follows.

$$\phi = \frac{\zeta}{g}\frac{d\log g}{dz} = \phi_1 + i\phi_2 \tag{38}$$

$$\ell + i\mathcal{S} = \frac{G\zeta}{\rho g} = e^{i(\theta-\omega)} \tag{39}$$

$$\ell = \cos(\theta-\omega) \ , \quad \mathcal{S} = \sin(\theta-\omega) \tag{40}$$

$$\rho_x = G\ell, \quad \rho_y = G\mathcal{S}, \quad \theta_x = -\frac{G}{\rho}\mathcal{S}, \quad \theta_y = \frac{G}{\rho}\ell \tag{41}$$

$$x_\rho = \ell/G, \quad x_\theta = -\rho\mathcal{S}/G, \quad y_\rho = \mathcal{S}/G, \quad y_\theta = \rho\ell/G \tag{42}$$

$$\rho_x^2 + \rho_y^2 = G^2 \ , \quad x_\rho^2 + x_\theta^2/\rho^2 = 1/G^2 \tag{43}$$

$$G_\rho = G\phi_1/\rho \ , \quad G_\theta = -G\phi_2 \ , \quad \omega_\rho = \phi_2/\rho \ , \quad \omega_\theta = \phi_1 \tag{44}$$

$$ds^2 = \frac{1}{G^2}d\rho^2 + \frac{\rho^2}{G^2}d\theta^2 + j\tilde{y}^2 dx_3^2 \tag{45}$$

$$\nabla P = G(P_\rho \hat{i} + \frac{1}{\rho} P_\theta \hat{j}) \tag{46}$$

$$\nabla \times \vec{V} = \frac{G^2}{\rho}[(\frac{\rho v}{G})_\rho - (\frac{u}{G})_\theta] \tag{47}$$

$$\vec{V} \times \nabla \times \vec{V} = \frac{G^2}{\rho}[(\frac{\rho v}{G})_\rho - (\frac{u}{G})_\theta](v\hat{i} - u\hat{j}) \tag{48}$$

$$\nabla . \vec{V} = \frac{G^2}{\rho}[(\frac{\rho u}{G})_\rho + (\frac{v}{G})_\theta] + j\frac{V}{y} \tag{49}$$

$$e_{11} = G(u_\rho + \frac{v}{\rho}\phi_2) \ , \ e_{22} = \frac{G}{\rho}[v_\theta + u(1-\phi_1)] \ , \ e_{33} = j\frac{V}{y}$$
$$e_{12} = \frac{1}{2}G[v_\rho - \frac{v}{\rho}(1-\phi_1) + \frac{1}{\rho}(u_\theta - u\phi_2)] \tag{50}$$

$$D = \frac{G}{\rho}[-v(1-\phi_1) + u\phi_2] \tag{51}$$

$$E = \frac{G}{\rho}[u(1-\phi_1) + v\phi_2] + e_{33} \tag{52}$$

$$\Omega = G(v_\rho - \frac{1}{\rho}u_\theta) - D \tag{53}$$

$$\Delta = e_{11} + e_{22} + e_{33} \tag{54}$$

In this case, the Navier-Stokes equations become:

$$P_t + G(uP_\rho + \frac{v}{\rho}P_\theta) + \gamma G(u_\rho + \frac{v_\theta}{\rho}) + \gamma E = \frac{DS}{Dt}$$
$$u_t + G(uu_\rho + \frac{v}{\rho}u_\theta) + vD + G\theta P_\rho = (\frac{4}{3}G\Delta_\rho - \frac{G}{\rho}\Omega_\theta - j\frac{\ell}{y}\Omega)\frac{\theta}{pR_e}$$
$$v_t + G(uv_\rho + \frac{v}{\rho}v_\theta) - uD + \frac{G}{\rho}\theta P_\theta = (\frac{4}{3}\frac{G}{\rho}\Delta_\theta + G\Omega_\rho + j\frac{\ell}{y}\Omega)\frac{\theta}{pR_e} \tag{55}$$
$$S_t + G(uS_\rho + \frac{v}{\rho}S_\theta) = [(\gamma-1)\Phi + \frac{\gamma}{P_r}\nabla^2\theta]/(pR_e)$$

with Φ defined by (28) and

$$\nabla^2\theta = \frac{G^2}{\rho}\left(\theta_\rho + \rho\theta_{\rho\rho} + \frac{1}{\rho}\theta_{\vartheta\vartheta}\right) + jG\,\frac{\theta_\rho \ell + \theta_\vartheta \ell/\rho}{y} \qquad (56)$$

4. Computational plane

The ζ-plane, however, is not the computational plane. In most instances (and particularly for viscous flows, when boundary layers and shear layers are present), grid lines must concentrate in the regions of highest gradients. An efficient way for achieving an uneven partition of grid lines consists of using stretching functions, which essentially define a correspondence between η (or ρ) and a new variable, X, and between ξ (or ϑ) and a new variable, Y. The boundaries of the region to be computed in the physical plane should be made to correspond to the X=0, X=1 lines and to the Y=0, Y=1 lines, respectively. The computation is performed in the (X, Y) plane, using a rectangular grid with evenly spaced lines; it must be noted, however, that X=constant lines and Y=constant lines on the physical plane are generally not orthogonal to each other, since the boundaries are not necessarily represented by ξ=constant lines and η=constant lines, or by ρ=constant lines and ϑ=constant lines.

We will consider here two examples. In the first, the basic variables in the ζ-plane are ξ and η; two boundaries are defined by constant values of ξ and two boundaries are defined by values of η which depend on ξ and t, as well. It will be necessary, thus, to define Y not only as a function of η but of ξ and t, and to distinguish carefully between the time, t, in the physical plane (or in the ζ-plane) and the time, T, in the computational plane. Therefore, we will write:

$$\begin{aligned} X &= X(\xi) \\ Y &= Y(\xi,\eta,t) \\ T &= t \end{aligned} \qquad (57)$$

Letting

$$a_{11} = GuX_\xi \;,\quad a_{12} = \gamma GX_\xi \;,\quad b_{11} = Y_t + GuY_\xi + GvY_\eta \;,\quad b_{12} = \gamma GY_\eta$$
$$g_{11} = \gamma GY_\xi \;,\quad a_{21} = G\theta X_\xi \;,\quad h_2 = G\theta Y_\xi \;,\quad b_{21} = G\theta Y_\eta \tag{58}$$

and

$$F = [(\gamma-1)\Phi + \frac{\gamma}{P_r}\nabla^2\theta]/(pR_e) \tag{59}$$

$$c_1 = \gamma E - F$$
$$c_2 = vD - \frac{\theta}{pR_e}[\frac{4}{3}G\Delta_\xi - G\Omega_\eta - j\frac{\ell}{y}\Omega] \tag{60}$$
$$c_3 = -uD - \frac{\theta}{pR_e}[\frac{4}{3}G\Delta_\eta + G\Omega_\xi + j\frac{\ell}{y}\Omega]$$

the equations of motion are recast in the form:

$$P_T + a_{11}P_X + b_{11}P_Y + a_{12}u_X + g_{11}u_Y + b_{12}v_Y + c_1 = 0$$
$$u_T + a_{11}u_X + b_{11}u_Y + a_{21}P_X + h_2P_Y + c_2 = 0 \tag{61}$$
$$v_T + a_{11}v_X + b_{11}v_Y + b_{21}P_Y + c_3 = 0$$
$$S_T + a_{11}S_X + b_{11}S_Y = F$$

In the second example, the basic variables in the ζ-plane are ρ and θ; two boundaries are defined by constant values of θ and two boundaries are defined by values of ρ which depend on θ and t. It will be necessary, thus, to define X not only as a function of ρ but of θ and t; therefore, we will write:

$$X = X(\rho,\theta,t)$$
$$Y = Y(\theta) \tag{62}$$

Computational plane

$$T = t$$

Letting

$$a_{11} = X_t + GuX_\rho + GvX_\theta/\rho \ , \quad a_{12} = \gamma GX_\rho \ , \quad b_{11} = GvY_\theta/\rho$$

$$b_{12} = \gamma GY_\theta/\rho \ , \quad g_{12} = \gamma GX_\theta/\rho \ , \quad a_{21} = G\theta X_\rho \tag{63}$$

$$h_3 = G\theta X_\theta/\rho \ , \quad b_{21} = G\theta Y_\theta/\rho$$

and F, c_1 as above in (59) and (60), respectively, and

$$c_2 = vD - \frac{\theta G}{pR_e}\left[\frac{4}{3}\Delta_\rho - \Omega_\theta/\rho - j\frac{\ell}{Gy}\Omega\right]$$

$$c_3 = -uD - \frac{\theta G}{pR_e}\left[\frac{4}{3}\Delta_\theta/\rho + \Omega_\rho + j\frac{\ell}{Gy}\Omega\right] \tag{64}$$

the equations of motion are recast in the form:

$$P_T + a_{11}P_X + b_{11}P_Y + a_{12}u_X + b_{12}v_Y + g_{12}v_X + c_1 = 0$$

$$u_T + a_{11}u_X + b_{11}u_Y + a_{21}P_X + c_2 = 0$$

$$v_T + a_{11}v_X + b_{11}v_Y + b_{21}P_Y + h_3P_X + c_3 = 0 \tag{65}$$

$$S_T + a_{11}S_X + b_{11}S_Y = F$$

It is easy to see that the first three equations (61) and the first three equations (65) have the same form as Equations (23) of [3]. The integration procedure explained in [3] can be applied. We expect the integration technique to provide a very good estimate of convection and wave-propagation effects which are common to inviscid and viscous flows.

5. Rigid boundaries

For a viscous flow, the velocity at a rigid boundary is assumed to vanish. There are no difficulties, thus, in the determination of u and v. Pressure and entropy require more care. We consider here the case of an isothermal wall; the temperature, θ is a prescribed constant. Because of (4), P and S are linearly related; therefore,

$$\frac{DS}{DT} = (1-\gamma)\frac{DP}{DT}$$

and consequently, the first of (36) and the first of (55) must be replaced by

$$P_t + G(uP_\xi + vP_\eta) + G(u_\xi + v_\eta) = 0 \tag{66}$$

and

$$P_t + G(uP_\rho + \frac{v}{\rho}P_\theta) + G(u_\rho + \frac{1}{\rho}v_\theta) = 0 \tag{67}$$

respectively, having taken into account that, in both cases, E vanishes identically. The equations to be solved are still (61) and (65), provided that a_{12}, b_{12}, g_{11} and g_{12} are divided by γ and c_1 is set equal to zero.

Once the pressure has been determined, S is obtained from (4). Therefore, S is not calculated directly as a result of dissipation and heat transfer in the flow, because the condition of constant wall temperature implies some external action, and (4) gives us the final outcome of such action and the local variation of pressure.

6. Integration procedure

The equations of motion (61) or (65) are integrated following the general guidelines of Section 6 in [3]. We define

$$C_1^X = g_{11}u_Y + c_1 \ , \quad C_2^X = b_{11}u_Y + h_2P_Y + c_2$$

$$C_1^Y = g_{12} v_X \quad , \quad C_2^Y = a_{11} v_X + h_3 P_X + c_3 \tag{68}$$

After finding the characteristic slopes, λ_i^X, λ_i^Y (i=1,2) from

$$\begin{vmatrix} a_{11}-\lambda_i^X & a_{21} \\ a_{12} & a_{11}-\lambda_i^X \end{vmatrix} = 0 \ , \quad \begin{vmatrix} b_{11}-\lambda_i^Y & b_{21} \\ b_{12} & b_{11}-\lambda_i^Y \end{vmatrix} = 0 \tag{69}$$

and letting

$$A_i = \frac{a_{11}-\lambda_i^X}{\lambda_2^X-\lambda_1^X} \ , \ B_i = \frac{b_{11}-\lambda_i^Y}{\lambda_2^Y-\lambda_1^Y}$$

$$D_{ij}^X = \frac{a_{ij}}{\lambda_2^X-\lambda_1^X} \ , \ D_{ij}^Y = \frac{b_{ij}}{\lambda_2^Y-\lambda_1^Y} \tag{70}$$

the equations to be integrated are:

$$\begin{aligned} P_T^X + A_1\lambda_1^X P_{X1} - A_2\lambda_2^X P_{X2} + D_{12}^X(\lambda_2^X u_{X2} - \lambda_1^X u_{X1}) + C_1^X = 0 \\ u_T + D_{21}^X(\lambda_2^X P_{X2} - \lambda_1^X P_{X1}) + A_1\lambda_2^X u_{X2} - A_2\lambda_1^X u_{X1} + C_2^X = 0 \end{aligned} \tag{71}$$

and

$$\begin{aligned} P_T^Y + B_1\lambda_1^Y P_{Y1} - B_2\lambda_2^Y P_{Y2} + D_{12}^Y(\lambda_2^Y v_{Y2} - \lambda_1^Y v_{Y1}) + C_1^Y = 0 \\ v_T + D_{21}^Y(\lambda_2^Y P_{Y2} - \lambda_1^Y P_{Y1}) + B_1\lambda_2^Y v_{Y2} - B_2\lambda_1^Y v_{Y1} + C_2^Y = 0 \end{aligned} \tag{72}$$

with

$$P_T = P_T^X + P_T^Y \tag{73}$$

For discretization, the space derivatives are classified into three categories: (i) the ones explicitly appearing in (71) and (72), (ii) the ones explicitly appearing in (68), and (iii) the ones appearing in (59), (60) and (64). The derivatives of the first category are discretized according to the rules (14)

and (15) of [3]; the derivatives of the second category according to the rules (34) and (35) of [3]; an the derivatives of the third category are approximated by ordinary centered differences, because the physical nature of the terms which they affect is diffusion. Few exceptions to the general rules are necessary for points on rigid boundaries or next to rigid boundaries. For points on rigid boundaries, the alternate two-point-three-point approximation is always taken using points inside the flow field. For points next to rigid boundaries, if use of a point located behind the wall were required in a three-point approximation, the latter is substituted by a two-point formula.

7. Numerical treatment of shocks

Shocks are generally present in a compressible flow field, either as boundaries or imbedded in the flow. In both cases, they can be treated numerically in the general framework of the computational technique described in the previous Sections. We begin with some general considerations.

Let $\hat{N}$ and $\hat{\tau}$ be the unit vector normal and tangential to a shock at any of its points, Q, respectively:

$$\hat{N} = N_1\hat{i} + N_2\hat{j} \quad , \qquad \hat{\tau} = -N_2\hat{i} + N_1\hat{j} \tag{74}$$

$\vec{W}$ the shock velocity,

$$\vec{W} = W\,\hat{N} \tag{75}$$

and $\tilde{u}$, $\tilde{v}$ the velocity components along $\hat{N}$ and $\hat{\tau}$, respectively:

$$\begin{aligned} \tilde{u} &= uN_1+vN_2 & u &= \tilde{u}N_1-\tilde{v}N_2 \\ \tilde{v} &= -uN_2+vN_1 & v &= \tilde{u}N_2+\tilde{v}N_1 \end{aligned} \tag{76}$$

The N-component of the velocity relative to the shock is

$$\tilde{u}_{rel} = \tilde{u} - W \tag{77}$$

The relative normal Mach number on the low pressure side of the shock is

$$M^2_{n\,1rel} = \frac{\tilde{u}^2_{1rel}}{\gamma\theta_1} \tag{78}$$

The Rankine-Hugoniot conditions are:

$$P_2 = P_1 + 1n\frac{2\gamma M^2_{n\,1rel} - \gamma + 1}{\gamma + 1}$$
$$\tilde{u}_{2rel} = \frac{\gamma - 1}{\gamma + 1}\tilde{u}_{1rel} + \frac{2}{\gamma + 1}\frac{\gamma\theta_1}{\tilde{u}_{1rel}} \tag{79}$$

We will need the derivatives of P_2 and u_{2rel} with respect to W:

$$\frac{\partial P_2}{\partial W} = -\frac{4\tilde{u}_{1rel}}{2\tilde{u}^2_{1rel} - (\gamma - 1)\theta_1}$$
$$\frac{\partial \tilde{u}_{2rel}}{\partial W} = -\frac{\gamma - 1}{\gamma + 1} + \frac{2}{\gamma + 1}\frac{\gamma\theta_1}{\tilde{u}^2_{1rel}} \tag{80}$$

Let us assume that the shock is oriented in the general direction of the X=constant lines; therefore, it can be defined by its intersections, X_s, with Y=constant lines. At each intersection, we consider two points, one on the low-pressure side and the other on the high-pressure side. The point on the low-pressure side must be updated by using information proceeding from that side only. The point on the high-pressure side must be updated by using information from both sides. The information proceeding from the low-pressure side must satisfy the Rankine-Hugoniot conditions; the information proceeding from the high-pressure side is carried to the shock along a characteristic. The acceleration of the shock results from the compatibility of

the different information. To obtain the characteristic equation, we should rewrite the equations of motion in a frame relative to the moving shock, where the Y-coordinate of the shock is unchanged but its X-coordinate follows the shock in its motion. Therefore, we will introduce a new set of coordinates,

$$\begin{aligned} \chi &= X - X_s(Y,T) \\ \varepsilon &= Y \\ \tau &= T \end{aligned} \tag{81}$$

and rewrite (61) and (65) in the form:

$$\begin{aligned} &P_\tau + \alpha_{11} P_\chi + b_{11} P_\varepsilon + \alpha_{12} u_\chi + b_{12} v_\varepsilon + \gamma_{12} v_\chi + c_1 = 0 \\ &u_\tau + \alpha_{11} u_\chi + b_{11} u_\varepsilon + \alpha_{21} P_\chi + h_2 P_\varepsilon + c_2 = 0 \\ &v_\tau + \alpha_{11} v_\chi + b_{11} v_\varepsilon + b_{21} P_\varepsilon + \eta_3 P_\chi + c_3 = 0 \\ &S_\tau + \alpha_{11} S_\chi + b_{11} S_\varepsilon = F \end{aligned} \tag{82}$$

where

$$\begin{aligned} &\alpha_{11} = a_{11} - b_{11} X_{sY} - X_{sT} \;,\quad \alpha_{12} = a_{12} - g_{11} X_{sY} \;,\quad \alpha_{21} = a_{21} - h_2 X_{sY} \\ &\gamma_{12} = g_{12} - b_{12} X_{sY} \;,\quad \eta_3 = h_3 - b_{21} X_{sY} \end{aligned} \tag{83}$$

A characteristic equation may now be obtained, using χ and τ as basic independent variables:

$$(\alpha_{11} - \lambda)(P_\tau + \lambda P_\chi) - \alpha_{12}(u_\tau + \lambda u_\chi) - \gamma_{12}(v_\tau + \lambda v_\chi) + R = 0 \tag{84}$$

where λ is the solution of the equation

$$\begin{vmatrix} \alpha_{11} - \lambda & \alpha_{21} & \eta_3 \\ \alpha_{12} & \alpha_{11} - \lambda & 0 \\ \gamma_{12} & 0 & \alpha_{11} - \lambda \end{vmatrix} = 0 \tag{85}$$

that is,

$$\lambda = \alpha_{11} \pm (\alpha_{12}\alpha_{21} + \gamma_{12}\eta_3)^{1/2} \tag{86}$$

and R comprises all the remaining terms.

Note now that

$$\begin{aligned} \alpha_{12} &= \gamma G \nu N_1 , \quad \gamma_{12} = \gamma G \nu N_2 \\ \alpha_{21} &= G\theta\nu N_1 , \quad \eta_3 = G\theta\nu N_2 \end{aligned} \tag{87}$$

where

$$\nu = \frac{(\alpha_{12}^2 + \gamma_{12}^2)^{1/2}}{\gamma G} \tag{88}$$

Therefore,

$$\begin{aligned} \alpha_{12} u + \gamma_{12} v &= \gamma G \nu \tilde{u} \\ \alpha_{12} u_\tau + \gamma_{12} v_\tau &= \gamma G \nu \tilde{u}_\tau - \gamma G \nu (u N_{1\tau} + v N_{2\tau}) \\ \alpha_{12} u_x + \gamma_{12} v_x &= \gamma G \nu \tilde{u}_x \end{aligned} \tag{89}$$

Instead of (84) we can write:

$$(\alpha_{11} - \lambda)(P_\tau + \lambda P_x) - \gamma G \nu (\tilde{u}_\tau + \lambda \tilde{u}_x) + R_1 = 0 \tag{90}$$

where

$$R_1 = R + \gamma G \nu (u N_{1\tau} - v N_{2\tau})$$

A further simplification is obtained by observing that

$$-\frac{\alpha_{11} - \lambda}{\gamma G \nu} = \pm \frac{(\alpha_{12}\alpha_{21} + \gamma_{12}\eta_3)^{1/2}}{\gamma G \nu} = \pm \frac{a}{\gamma} \tag{91}$$

because of (87) and (88), so that (90) can be written in the form:

$$\pm\frac{a}{\gamma}(P_\tau+\lambda P_x)+\tilde{u}_\tau+\lambda\tilde{u}_x+R_1=0 \tag{92}$$

The values of P_τ and $\tilde{u}_\tau$, obtained by integrating the Navier-Stokes equations (82) using information from the high-pressure side of the shock only, must satisfy (92). On the other hand, the exact solution of the flow problem in the presence of the shock, which accounts also for the information from the low-pressure side and the Rankine-Hugoniot conditions, must satisfy (92) as well. Therefore, if we write (92) twice, once for the τ-derivatives as obtained from the Navier-Stokes equations (that is, using for the shock point the same integration procedure which is applied to other points) and again for the exact τ-derivatives and we subtract one equation from the other, the simple result is obtained:

$$\pm\frac{a}{\gamma}(P_\tau-P_\tau^{(NS)})+\tilde{u}_\tau-\tilde{u}_\tau^{(NS)}=0 \tag{93}$$

where the derivatives obtained from the Navier-Stokes equations are labeled (NS) and the exact derivatives are unlabeled.

The latter derivatives can obviously be expressed in the form:

$$P_\tau=P_\tau^*+\frac{\partial P_2}{\partial W}W_\tau\,,\quad \tilde{u}_\tau=\tilde{u}_\tau^*+\frac{\partial\tilde{u}_2}{\partial W}W_\tau \tag{94}$$

where f_τ^* is a derivative computed considering W as a constant. The acceleration of the shock is thus obtained:

$$W_\tau=\frac{\pm a(P_\tau^{(NS)}-P_\tau^*)+\gamma(\tilde{u}_\tau^{(NS)}-\tilde{u}_\tau^*)}{\pm a\,\partial P_2/\partial W+\gamma\,\partial\tilde{u}_2/\partial W} \tag{95}$$

Since both the starred derivatives and the derivatives indicated by (NS) are computed using the same initial values, (95) can be replaced by

$$W_\tau\Delta t=\frac{\pm a(P^{(NS)}-P^*)+\gamma(\tilde{u}^{(NS)}-\tilde{u}^*)}{\pm a\,\partial P_2/\partial W+\gamma\,\partial\tilde{u}_2/\partial W} \tag{96}$$

where P^* and $\tilde{u}^*$ are the values on the high-pressure side of the shock obtained from updated values on the low-pressure side by applying the Rankine-Hugoniot conditions to a shock whose geometry has been updated but whose velocities, W, are still the same as at the beginning of the integration step. This result [4] is remarkable since it provides an extremely simple method for calculating the shock acceleration although it relies on the same basic concepts which have been shown to be necessary for a proper, physically correct, handling of shocks [5].

We will now consider first the case where the shock is a boundary, moving into a gas at rest, and then the case of an imbedded shock.

In the case of a shock moving into a gas at rest, let us assume that the shock is a right boundary of the computational field. It is, thus, defined by X=1; in this case, χ, ε and τ coincide with X, Y and T, respectively and $\alpha_{11}=a_{11}$, $\alpha_{21}=a_{21}$, $\alpha_{12}=a_{12}$, $\gamma_{12}=g_{12}$, $\eta_3=h_3$. The characteristic reaching the shock from the high-pressure side is a right-running characteristic, and in the preceding equations, whereas a $\pm$ appears, the upper sign must be used. Note in addition that $\tilde{u}_1=0$ and $\tilde{v}_1=0$; therefore, $\tilde{u}_{1rel}=-W$ and $M^2_{n1rel}=W^2/\gamma$. In this case, obviously, the low-pressure side values are known without any need for computing; the (NS)-values on the high-pressure side are obtained together with and using the same procedure as for interior grid points.

For an imbedded shock, whose location does not generally coincide with a grid line, we use a simplified procedure to obtain the values at the shock on the low-pressure side and the (NS) values on the high-pressure side. On the low-pressure side, instead of integrating (82) (which would require a special, and not easy, redefinition of approximations for the χ- and ε-derivatives), we simply assume that the values at the shock can be extrapolated from the two adjacent grid points on the same y=constant line, both at the end of the predictor and the corrector level. On the high-pressure side, we assume that the T-derivatives on the shock are equal to the T-derivatives at the grid point next to the shock on the same Y=constant line. Note, however, that

$$f_\tau = f_T + f_X X_{sT} \tag{97}$$

for any function f. The values of f_T at the shock are assumed to be the same as at the next grid point on the hight-pressure side, on the same Y=constant line. The values of f_X are approximated as follows:

$$f_X = [f_A - f_s + \frac{1-\epsilon}{1+\epsilon}(f_B - f_s)]/\Delta X \tag{98}$$

where $\epsilon = (X_A - X_s)/\Delta X$ and A is the grid point next to the shock on the high-pressure side and B is the next grid point. This formula provides a smooth transition when the shock crosses an X=constant line.

For an imbedded shock, thus, the calculation proceeds as follows: In the predictor stage, after updating all grid points, the low-pressure side of the shock is obtained by extrapolation and (97) is also applied to P, u, v and S. The values on the high-pressure side are updated by adding $f_\tau \Delta t$ to the initial values of f; the values so obtained are the predicted $f^{(NS)}$. The predicted f^* are obtained by applying (79) to the predicted values on the low-pressure side. Then, (96) is applied and W is temporarily updated, but its original value is retained in storage. The geometry of the shock is updated, considering that, in virtue of (75), (14) and (19),

$$\xi_{st} = G\, W/N_1 \tag{99}$$

or, using (41) in lieu of (14),

$$\rho_{st} = G\, W/N_1 \tag{100}$$

and using the approximations:

$$\begin{aligned} \xi_s(t+\Delta t) &= \xi_s(t) + \xi_{st}\Delta t + \frac{1}{2}\xi_{stt}\Delta t^2 \\ \rho_s(t+\Delta t) &= \rho_s(t) + \rho_{st}\Delta t + \frac{1}{2}\rho_{stt}\Delta t^2 \end{aligned} \tag{101}$$

where the second derivatives are obtained by differentiating (99) or (100). In the corrector stage, the procedure outlined above for the predictor stage is repeated through the application of

(97). The updating of the values on the high-pressure side is obtained by adding

$$\frac{1}{2}(f_\tau - f_\tau^{(pred)})\Delta t$$

to the predicted values. The corrected f* are obtained by applying (79) to the corrected values on the low-pressure side, with the original value of W. Then, (96) is applied again and W is definitively updated. The Rankine-Hugoniot conditions (79) are applied once more to the corrected values on the low-pressure side using the final value of W, to obtain the final values on the high-pressure side. The entropy is also computed from

$$S_2 = S_1 + P_2 - P_1 - \gamma \ln(\tilde{u}_{1rel}/\tilde{u}_{2rel}) \qquad (102)$$

At this stage, it is convenient to correct the values at the grid point next to the shock on the high-pressure side. Pressure and velocity components are interpolated from the values at the shock and the following grid point. Entropy is also interpolated considering that it is carried along a streamline.

8. An example

To illustrate the technique, let us consider the following example. A duct (either two-dimensional or axisymmetric) has its centerline on the x-axis; its lower wall (AC) is defined as the image, in the z-plane, of a straight line, $\theta=\theta_o$, in the ζ-plane (Fig. 1). The mapping is defined by

$$z = (r_o/\pi)[(z_2^2 - 1/z_2^2)/2 - \log z_2^2 - i\pi]$$
$$z_2 + 1/z_2 = 2B(\zeta + 1/\zeta) \qquad (103)$$

where r_o is an arbitrary parameter, and B is determined to assure correspondence between $\zeta=1$ and $z=-i$. The section of the duct at $x=0$ (AB) is defined by $\rho=1$. We assume that the duct itself is fitted to an extremely long shock tube in which, by means of an ideal device, the flow behind the shock is made to arrive to the

exit without a sizeable boundary layer and practically uniform

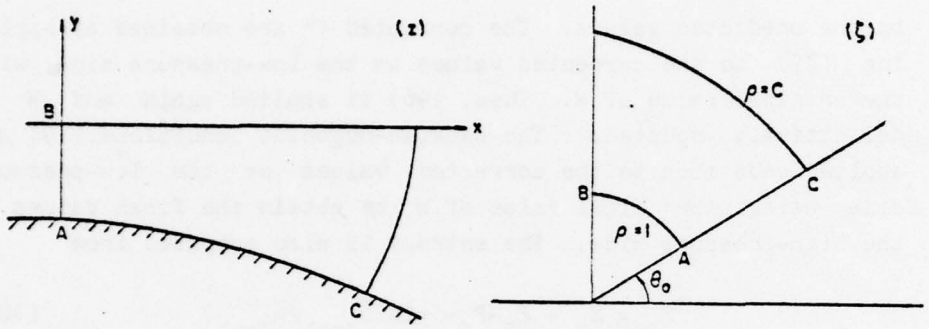

Fig. 1

across, save for the vanishing of the velocity on the wall. At t=0, the shock (which we will call the precursor shock) is just out of the shock tube and into the duct. At every value of t, we will define its position as

$$c = \rho(\theta,t) \tag{104}$$

and we will compute the flow in the duct (that is, between $\rho=1$ and $\rho=c$ and between $\theta=\theta_o$ and $\theta=\pi/2$) assuming that the supersonic flow at the entrance of the duct remains unchanged.

The computational variables X, Y and T are defined in terms of ρ, θ and t as follows:

$$\theta = (\frac{\pi}{2} - \theta_o)\frac{\tanh[\alpha(Y-1)]}{\tanh\,\alpha} + \frac{\pi}{2}$$

$$\rho = 1 + [c(Y,T) - 1]X \tag{105}$$

$$t = T$$

An example

The calculation is started at a small, positive value of t, when the precursor shock has already moved from AB. Initially, the shock is assumed to lie on a ρ=constant line (with the value of the constant, c_o, slightly greater than 1), and all parameters pertinent to the shock are assumed equal to their values at t=0 (since the flow behind the shock is uniform, the shock Mach number defines pressure, velocity and entropy). Uniform flow is assumed between AB and the shock, if the gas is inviscid. The velocity component, v is made equal to zero throughout. Initially, the computational region is divided into two strips only along the X-axis. Along the Y-axis we consider as many partitions as necessary to provide sufficient resolution. Since the flow is viscous, we need some modifications to the initial conditions near the wall, to account for the vanishing of the velocity at the wall. The precursor shock cannot reach the wall; the perturbation front, elsewhere in the form of a shock, becomes a characteristic at the wall, somewhat smeared out by viscous diffusion. Therefore, on the initial ρ=c line which represents the shock, P is assumed equal to zero at the wall. On the next wall point, P is taken equal to one half of its value behind the shock. The wall temperature is assumed equal to 1 at any time. The entropy is defined accordingly. The u-velocity component is taken equal to one half of its value behind the shock along the second θ=constant line from the wall. The calculation proceeds as detailed above. We note that the centerline is computed as a symmetry line, not as a rigid wall. For computational purposes, the shock geometry is prolonged to the wall with a constant value of c, and the wall point is computed as any interior, shockless point, taking advantage of the fact that the state of the gas in front of the perturbed region is known. The same procedure is automatically applied to any other point on the perturbation front, if the shock happens to lose its strength completely.

As the calculation proceeds, the number of grid intervals in the X-direction is doubled every time (c-1) on the centerline exceeds 1.4 times its initial value or the value it had at the

previous doubling, until the total number of intervals is 16.

Certain features of the flow are common to the inviscid and viscous models. An expansion appears from the beginning near the inlet of the duct; the region of maximum expansion moves from left to right, but at a slower speed than the precursor shock. Consequently, even with the precursor shock losing strength, the pressure behind it remains higher than the lowest pressure already attained along the duct. The particles are accelerated and then decelerated again. A compression wave appears, which tends to steepen up, as every compression wave does, and another shock results eventually.

In the presence of viscosity, the recompression wave and the secondary shock strongly interact with the boundary layer in the process of formation. The latter thickens and separates very soon. Between the main stream and the wall, a wide dead-water region appears, where the pressure tends to equalize the ambient pressure (in front of the precursor shock). When the separated flow becomes steady, it is what is commonly defined as a plume. From the separation point on, the plume is insensitive to the wall geometry and the flow inside it is essentially inviscid. The results of the calculation of a steady, inviscid flow in a plume can be used to judge whether the viscous calculation approaches its theoretical asymptote, and how well.

In the present example, $\alpha=2$, and the sector between $\theta=\theta_o$ and $\theta=\pi/2$ is divided into 16 intervals. Consequently, we obtain a fair accumulation of grid lines near the wall, and still work with a reasonably small number of lines. It is clear, however, that the resolution is well below the limits which are usually recommended for a good description of Reynolds number effects; the lack of an adequate resolution is particularly felt in the vicinity of the plume shear layer. Nevertheless, the present results are very encouraging, just because very good qualitative results are obtained with such a coarse mesh.

Based on realistic values of the inner diameter of the shock tube (25.4 mm), of the kinematic viscosity of air (.0016 m^2/sec) and of the speed of sound of the gas at rest (360 m/sec), R_e turns out to be of the order of 2500. For such a Reynolds number, the

resolution of the grid near the wall cannot provide accurate details of the boundary layer, such as needed, for example, to compute the skin friction, but it is sufficient to furnish an adequate picture of the layer in the general context of the flow.

The Prandtl number is taken equal to 1, and γ equal to 1.4. The values of r_o and θ_o are 2.2603 and 1.2, respectively. The temperature at the wall is assumed to be equal to 1, that is, to the temperature in the gas at rest. The value of P at the inlet is 1.6487. Consistent values of u and S are u=1.6551, S=0.1702. The Mach number at the inlet is barely supersonic, M=1.040. The flow is assumed to be two-dimensional.

The evolution of the flow is shown in Figs. 2 through 13. In Figs. 2 through 8, isobars are plotted. The left vertical line is the inlet cross-section, the lower curved line is the wall of the duct, the upper horizontal line is the duct centerline (on which notches indicate multiples of the unit length); and the right boundary is the precursor shock. The line marked with 0 is the sonic line. Step 800 is typical of the first phase of evolution, showing an accented minimum of pressure on the wall; velocity vectors drawn for that step indicate the beginning of recirculation in the boundary layer around the region of minimum pressure (Fig. 9). At step 1200, the minimum pressure has moved to the centerline, and a steepening up of the pressure, all across the duct, is evident. At step 1400, an imbedded shock is fitted (marked in the figure by +). The initial fitting of the shock is rather arbitrary, but such arbitrariness is not restrictive. In general, an imbedded shock is fitted on any θ=constant line, in the middle of an interval where the difference in P exceeds 0.6, as it is suppressed if its normal Mach number becomes less than 1 or if locally the shock stretches over more than two X-intervals over a single Y-interval.

Note that the computational technique allows the shock to end inside the flow field, and that isobars between the end-point of the shock and the wall shape up in a way which is, at least qualitatively, typical of shock-boundary-layer interactions. Velocity vectors at this step (Fig. 10) show a pronounced recir-

culation bubble.

At step 2400, the flow field is mostly subsonic; the supersonic flow is confined to a jet-like region (see Fig. 11, where lines of constant Mach number are shown, and the veocity vectors in Fig. 12).

At step 3400 the loss of accuracy consequent to loss of resolution is evident; the jet region, where the imbedded shock is still present, is covered by three mesh intervals only. The Mach number distribution (Fig. 13) has the correct trend, but the transversal gradient is spread out too widely. Nevertheless, note the formation of a transversal pressure gradient, very similar to the pattern found in the isobars computed for a steady plume originated by the same duct, with separation taking place exactly where the pressure at the wall equals the ambient pressure (Fig. 14).

To conclude, we show an impressive picture of streamlines at this step in Fig. 15.

9. References

1. R. W. MacCormack and H. Lomax, Numerical solution of compressible viscous flows, Ann. Rev. Fluid Mech., 11, 289, 1979

2. G. Moretti, Conformal mappings for computation of steady, three-dimensional, supersonic flows, Num./Labor. computer methods in fluid mechanics, ASME, 13, 1976

3. G. Moretti, The λ-scheme, Comp. and Fluids, 7,191, 1979

4. T. de Neef and G. Moretti, Shock fitting for everybody, to appear in Comp. and Fluids

5. G. Moretti, Thoughts and afterthoughts about shock computations, PIBAL Report No. 72-37, 1972

RUN 33, K,T= 200 0.3185, LINE= 1 DREF,LAST REF= 0.020 1.640

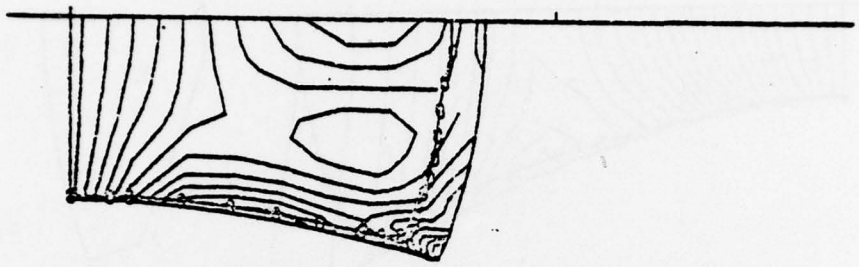

RUN 33, K,T= 400 0.6766, LINE= 1 DREF,LAST REF= 0.040 1.640

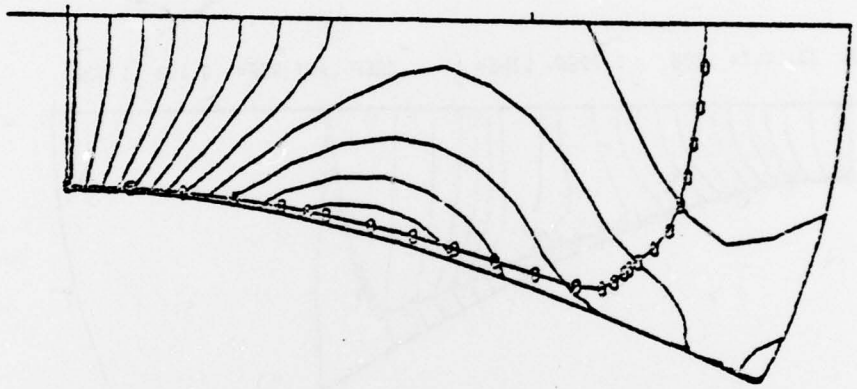

RUN 33, K,T= 600 1.0397, LINE= 1 DREF,LAST REF= 0.050 1.300

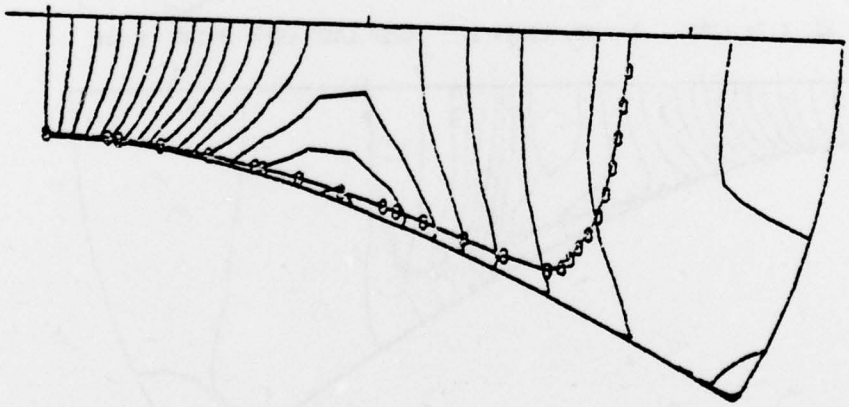

Fig. 2

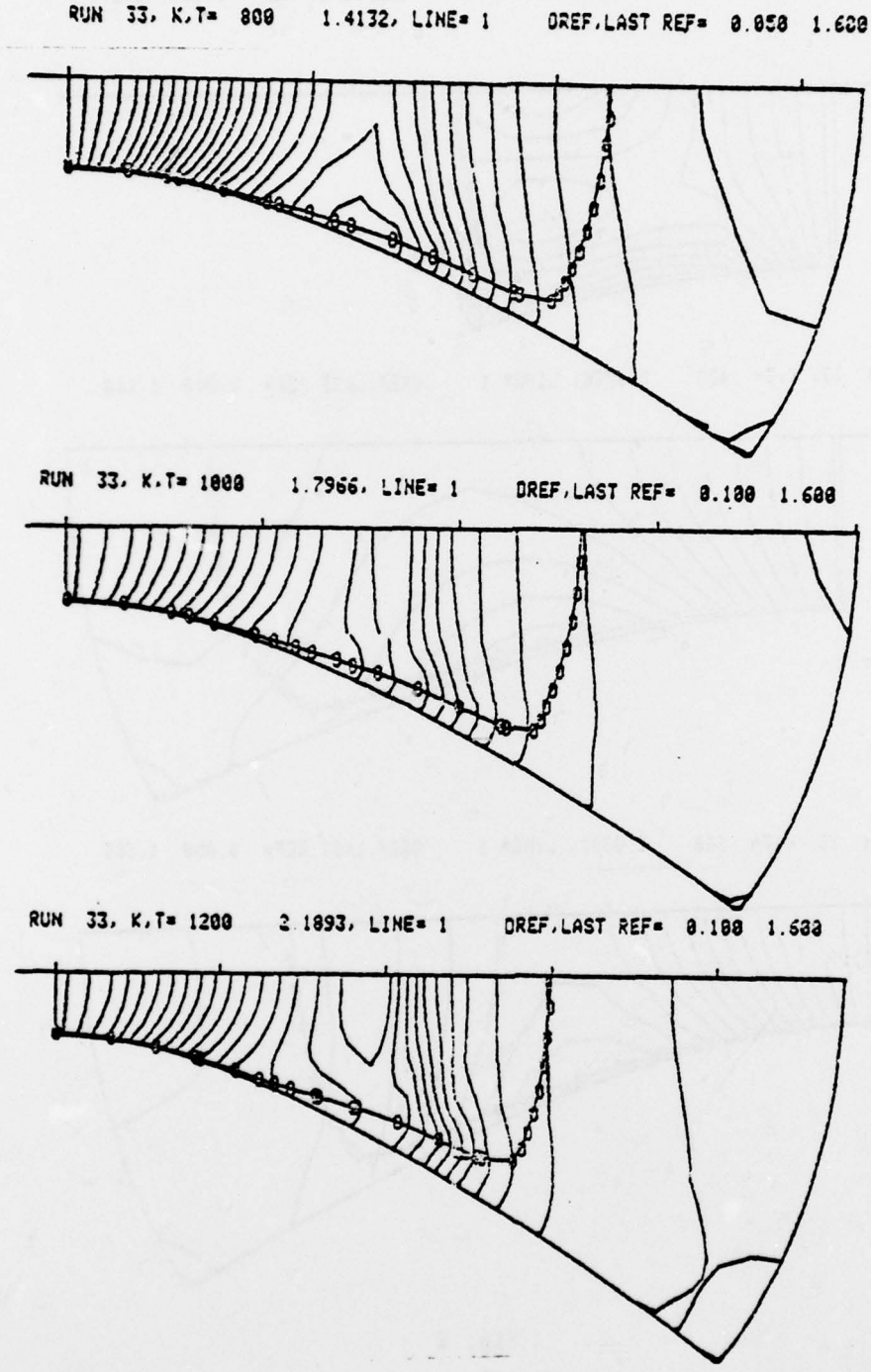
RUN 33, K,T= 800 1.4132, LINE= 1 DREF,LAST REF= 0.050 1.600
RUN 33, K,T= 1000 1.7966, LINE= 1 DREF,LAST REF= 0.100 1.600
RUN 33, K,T= 1200 2.1893, LINE= 1 DREF,LAST REF= 0.100 1.600

Fig. 3

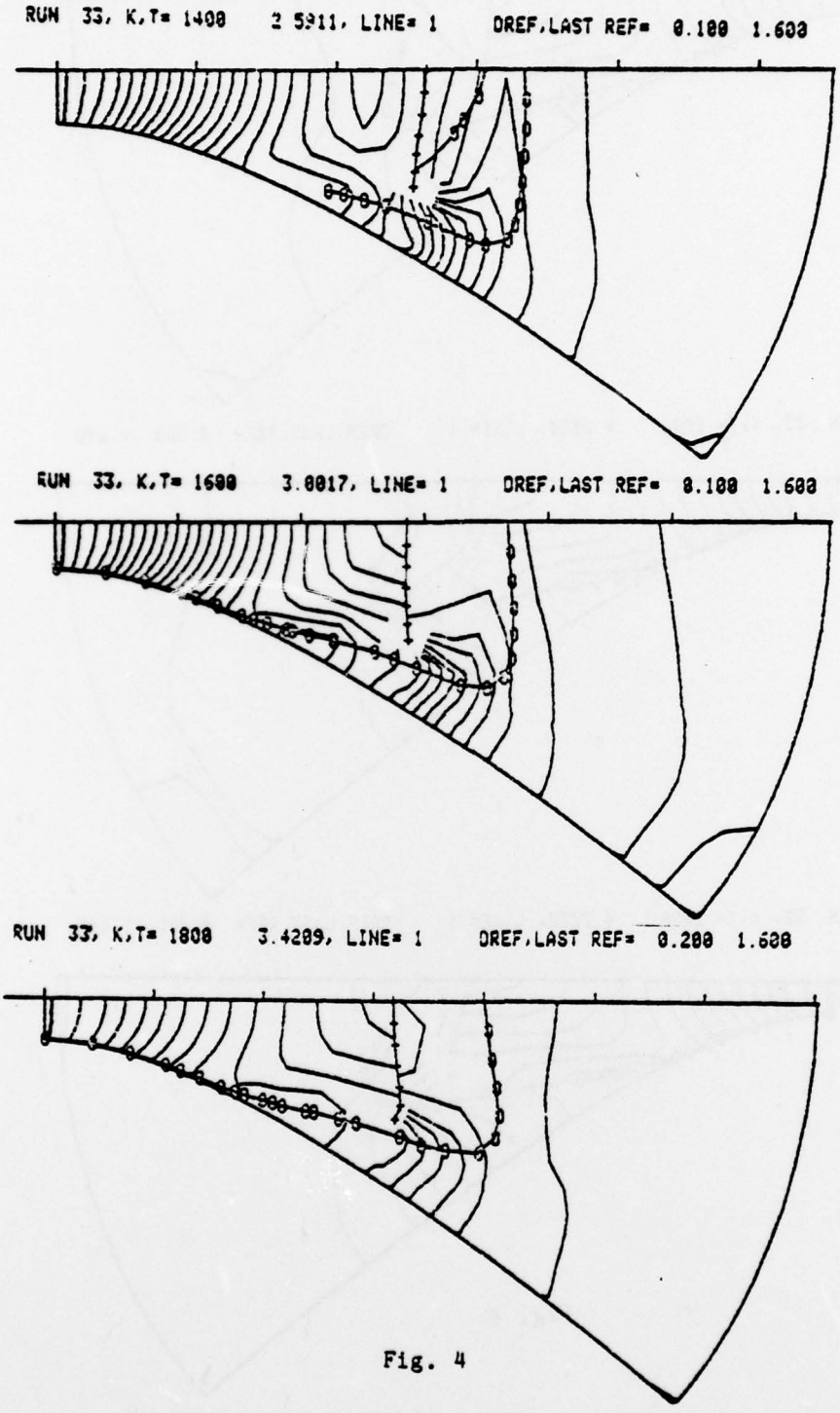
RUN 33, K,T= 1400 2.5911, LINE= 1 DREF,LAST REF= 0.100 1.600
RUN 33, K,T= 1600 3.0017, LINE= 1 DREF,LAST REF= 0.100 1.600
RUN 33, K,T= 1800 3.4209, LINE= 1 DREF,LAST REF= 0.200 1.600

Fig. 4

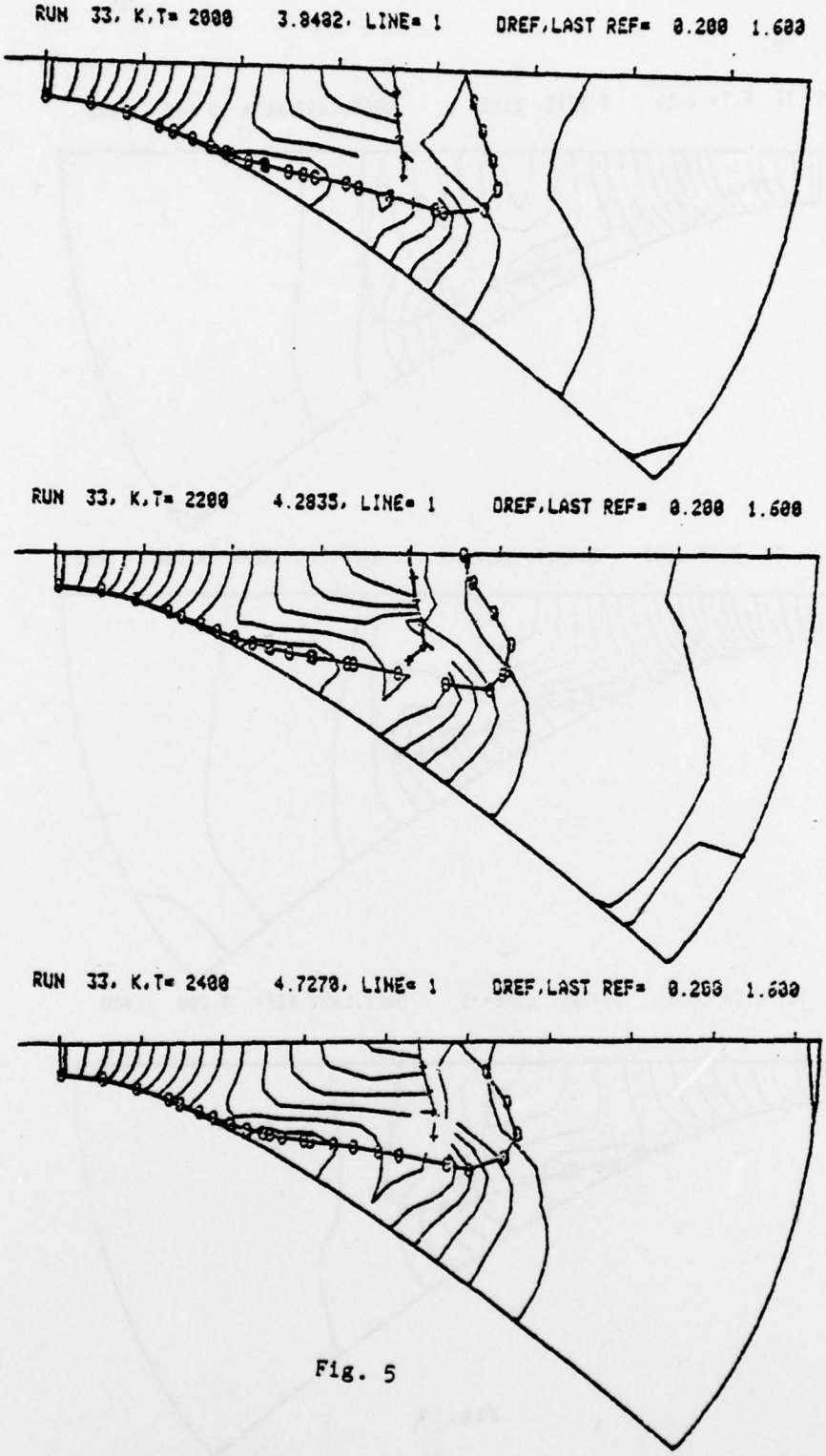
RUN 33, K,T= 2000 3.8402, LINE= 1 DREF,LAST REF= 0.200 1.600
RUN 33, K,T= 2200 4.2835, LINE= 1 DREF,LAST REF= 0.200 1.600
RUN 33, K,T= 2400 4.7270, LINE= 1 DREF,LAST REF= 0.200 1.600

Fig. 5

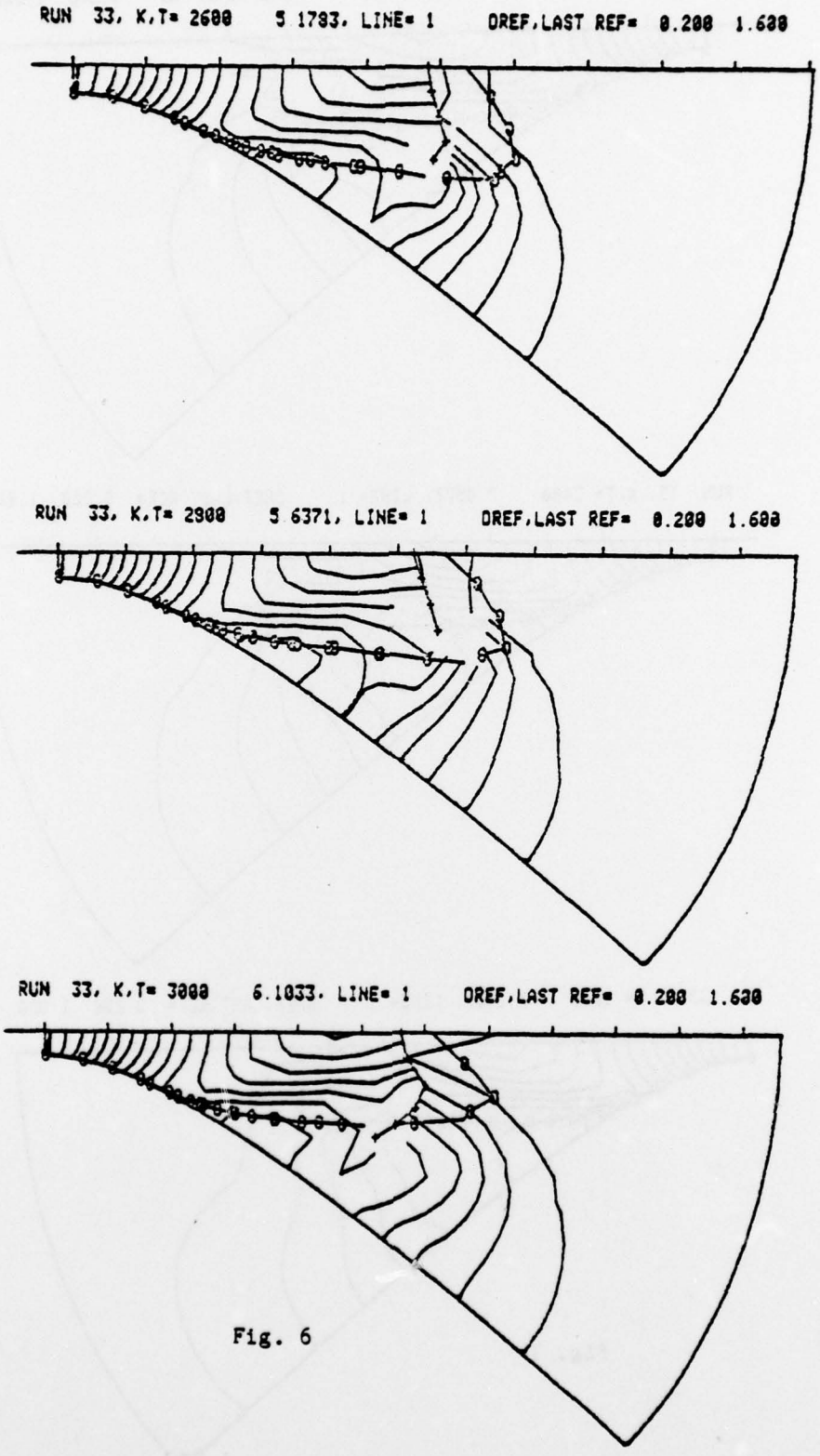
RUN 33, K,T= 2600 S 1793, LINE= 1 DREF,LAST REF= 0.200 1.600
RUN 33, K,T= 2900 S 6371, LINE= 1 DREF,LAST REF= 0.200 1.600
RUN 33, K,T= 3000 6.1033, LINE= 1 DREF,LAST REF= 0.200 1.600

Fig. 6

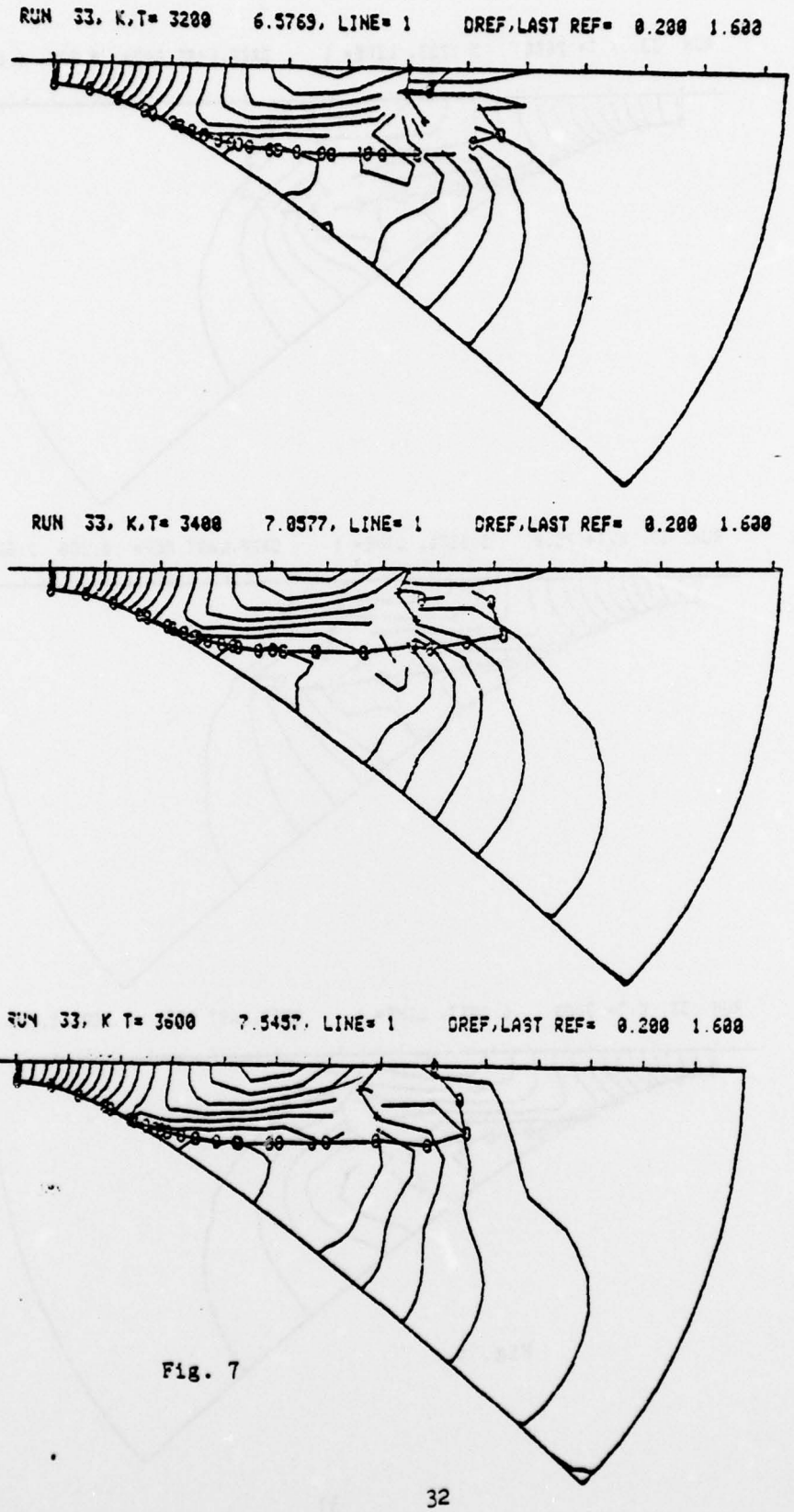
RUN 33, K,T= 3200 6.5769, LINE= 1 DREF,LAST REF= 0.200 1.600
RUN 33, K,T= 3400 7.0577, LINE= 1 DREF,LAST REF= 0.200 1.600
RUN 33, K T= 3600 7.5457, LINE= 1 DREF,LAST REF= 0.200 1.600

Fig. 7

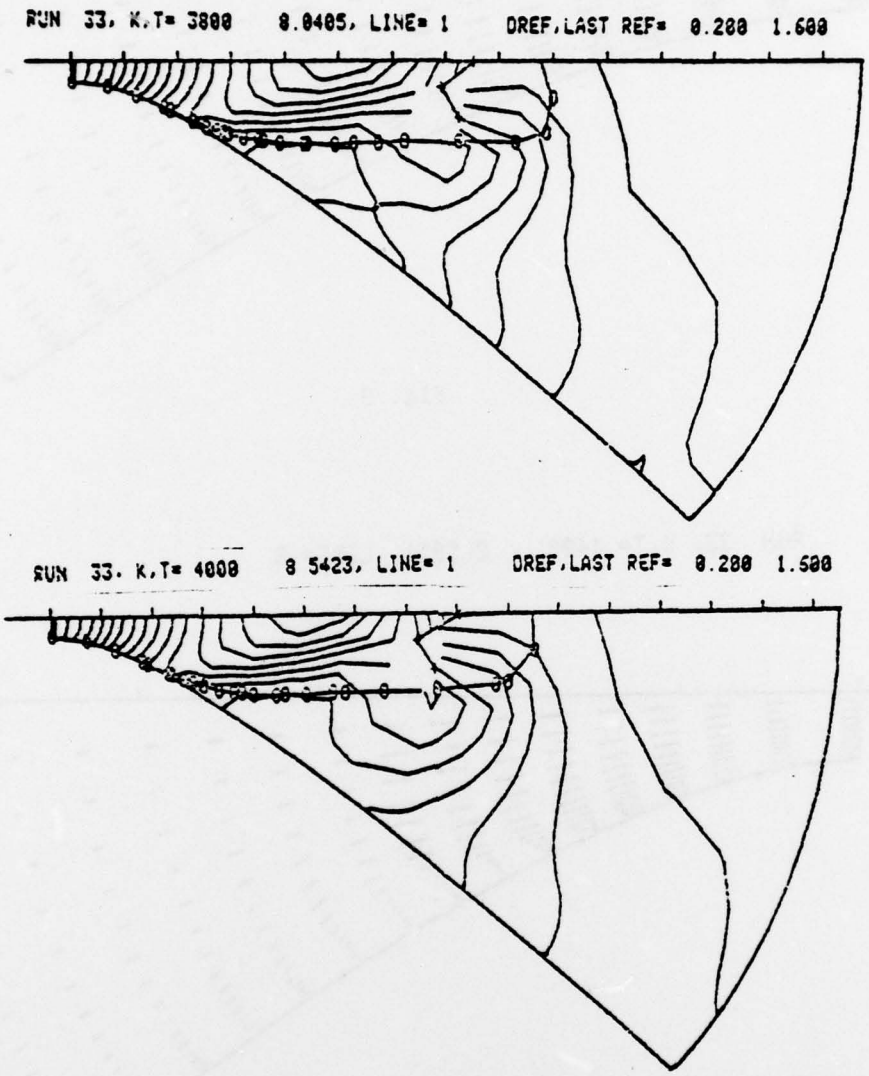
RUN 33. K,T= 3800 8.0405, LINE= 1 DREF,LAST REF= 0.200 1.600
RUN 33. K,T= 4000 8 5423, LINE= 1 DREF,LAST REF= 0.200 1.500

Fig. 8

RUN 33, K,T= 800 1.4132, LINE= 8

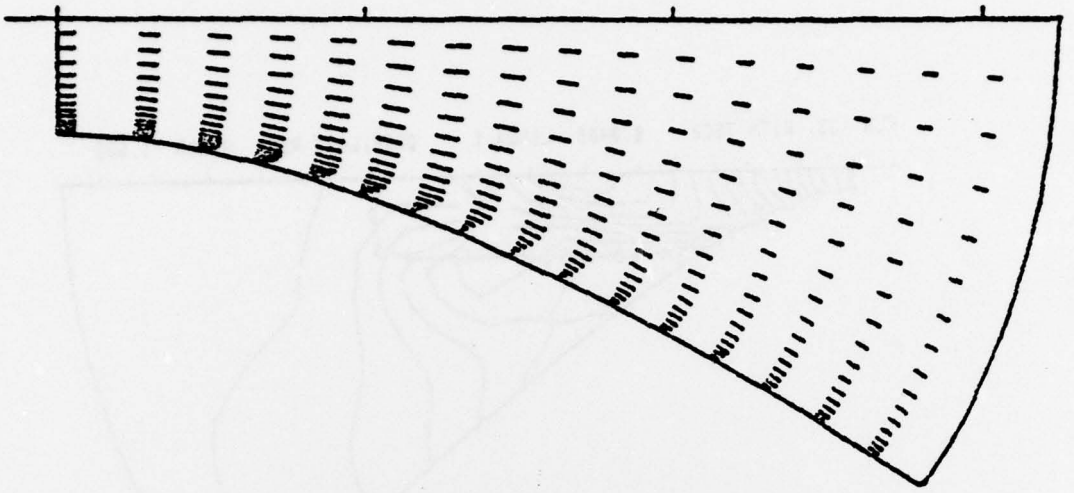

Fig. 9

RUN 33, K,T= 1400 2.5911, LINE= 8

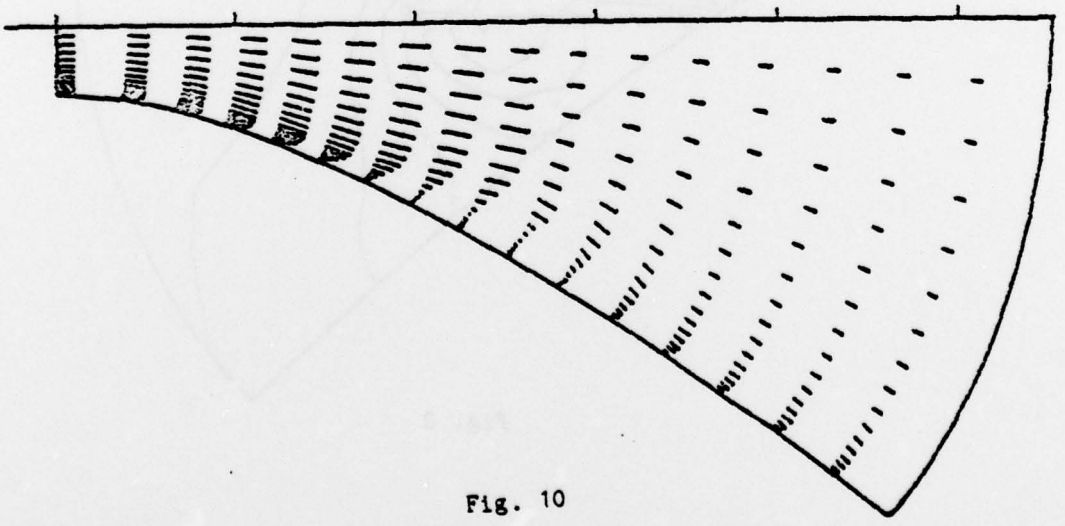

Fig. 10

RUN 33, K,T = 2400 4.7270, LINE = 2 DREF, LAST REF= 0.200 2.800

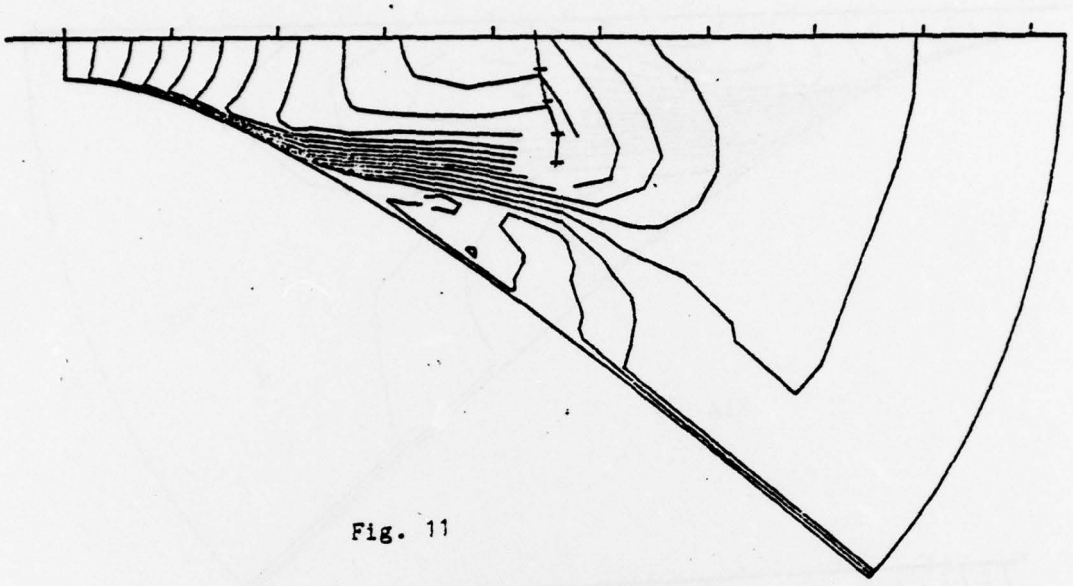

Fig. 11

RUN 33, K,T = 2400 4.7270, LINE = 8

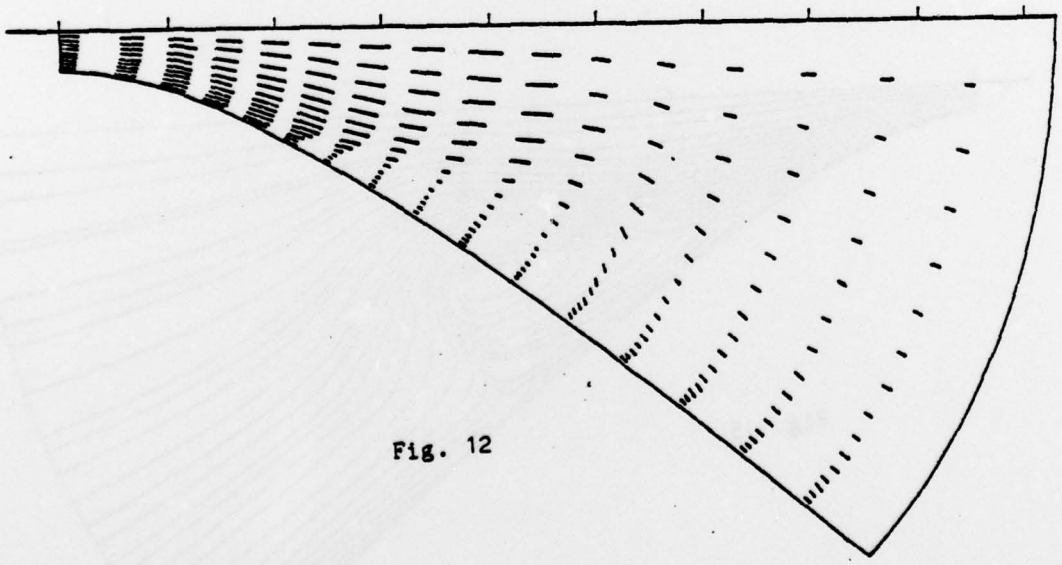

Fig. 12

RUN 33, K,T = 3400 7.0577, LINE = 2 DREF, LAST REF = 0.200 3.000

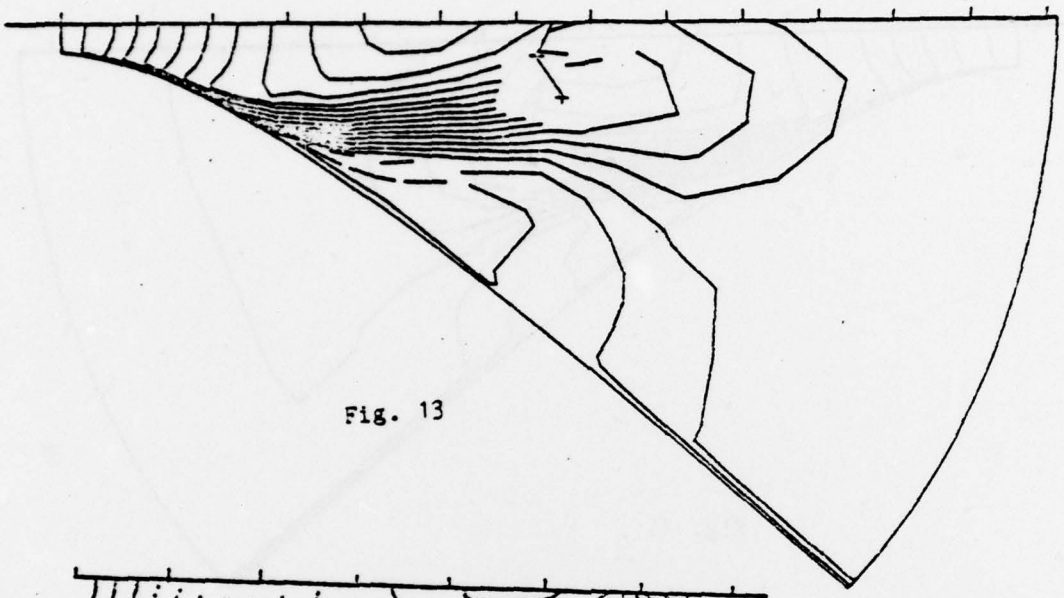

Fig. 13

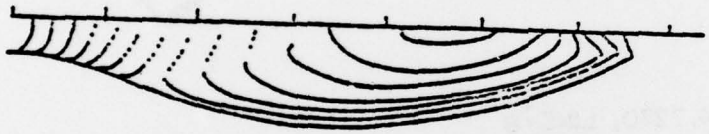

Fig. 14

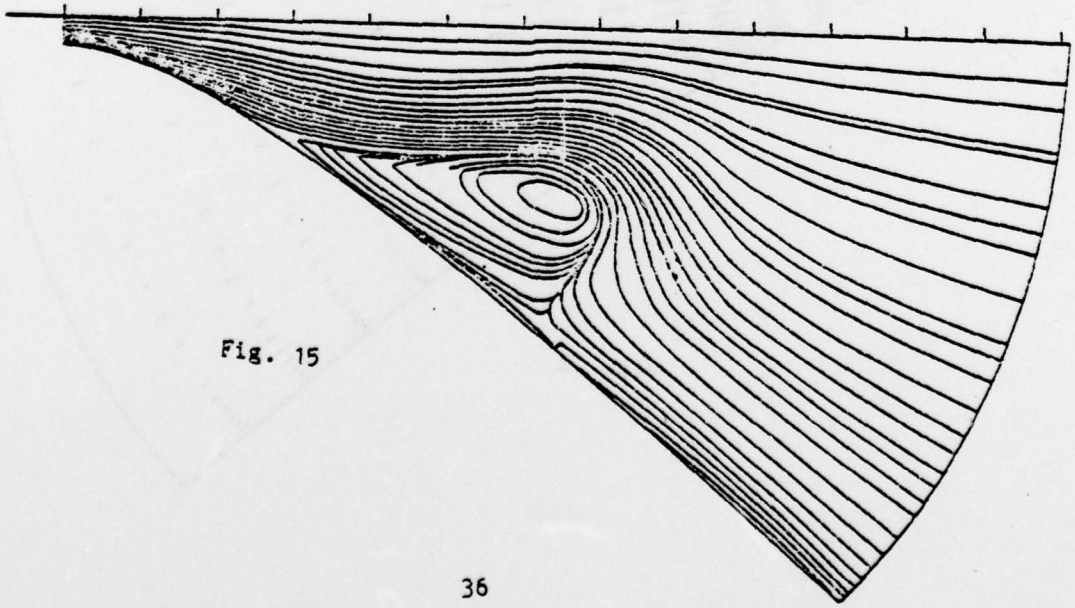

Fig. 15

Unclassified

SECURITY CLASSIFICATION OF THIS PAGE (When Data Entered)

REPORT DOCUMENTATION PAGE

READ INSTRUCTIONS BEFORE COMPLETING FORM

1. REPORT NUMBER: POLY M/AE Report No. 79-40
2. GOVT ACCESSION NO.
3. RECIPIENT'S CATALOG NUMBER (9)
4. TITLE (and Subtitle) (6): Numerical Integration of Compressible, Viscous Flow Equations.
5. TYPE OF REPORT & PERIOD COVERED: Scientific Interim rept.
6. PERFORMING ORG. REPORT NUMBER (15)
7. AUTHOR(s) (10): Gino Moretti
8. CONTRACT OR GRANT NUMBER(s): Grant No. DAAG 29-77-G-0072 Project P 14369-E
9. PERFORMING ORGANIZATION NAME AND ADDRESS: Polytechnic Institute of New York, Route 110, Farmingdale, New York 11735
10. PROGRAM ELEMENT, PROJECT, TASK AREA & WORK UNIT NUMBERS
11. CONTROLLING OFFICE NAME AND ADDRESS: U. S. Army Research Office, Post Office Box 12211, Research Triangle Park, NC 27709
12. REPORT DATE: Sept[redacted]79
13. NUMBER OF PAGES: 38
14. MONITORING AGENCY NAME & ADDRESS (if different from Controlling Office) (12) 38
15. SECURITY CLASS. (of this report): Unclassified
15a. DECLASSIFICATION/DOWNGRADING SCHEDULE: NA
16. DISTRIBUTION STATEMENT (of this Report): Approved for public release; distribution unlimited
(18) ARO (19) 14369.3-E
17. DISTRIBUTION STATEMENT (of the abstract entered in Block 20, if different from Report): NA
(14) POLY-M/AE-79-40
18. SUPPLEMENTARY NOTES: The findings in this report are not to be construed as an official Department of the Army position, unless so designated by other authorized documents
19. KEY WORDS (Continue on reverse side if necessary and identify by block number): Navier-Stokes equations; Numerical gas dynamics; Imbedded shocks; Unsteady viscous flow in ducts; lambda
20. ABSTRACT (Continue on reverse side if necessary and identify by block number): A method for integrating the Navier-Stokes equations numerically is given, which takes the most advantage of the (λ)-scheme for the integration of inviscid equations. Full details for suplementing the method (with the inclusion of imbedded shocks treatment) in two-dimensional unsteady flows are given. Results of one application are presented.

DD FORM 1 JAN 73 1473

Unclassified

SECURITY CLASSIFICATION OF THIS PAGE (When Data Entered)

410 338